INTRODUCTION TO HEAT TRANSFER TEST SETUP AND MANUFACTURING PROCESS FOR THE SCRAP RECEIVER

Matti Lubkoll[1], Thomas M Harms[2] and Theodor W von Backström[3]

[1] Solar Thermal Energy Research Group (STERG), Dept. Mechanical and Mechatronic Engineering, Stellenbosch University, South Africa; +27 (0)71 272 4775; matti@sun.ac.za

[2] Solar Thermal Energy Research Group (STERG), Dept. Mechanical and Mechatronic Engineering, Stellenbosch University, South Africa; tmh@sun.ac.za

[3] Solar Thermal Energy Research Group (STERG), Dept. Mechanical and Mechatronic Engineering, Stellenbosch University, South Africa; twvb@sun.ac.za

Abstract

The Spiky Central Receiver Air Pre-heater (SCRAP) receiver is a novel external metallic tubular central receiver concept. The SCRAP receiver is designed to increase an air-receiver's solar-to-thermal performance. This is aimed to be achieved by enhancing heat transfer to the pressurized air-stream within the absorber assemblies (spikes) by utilizing an internally finned tube geometry.

To validate the models predicting the pressurized air flow and heat transfer within a spike, an experimental test setup was designed, constructed and built at the heat transfer laboratories at Stellenbosch University. This work introduces the design of the test setup and presents the manufacturing of the internally finned components.

Keywords: CSP; Central Receiver; Pressurized Air Receiver; Experimental Setup; Heat Transfer

1. Introduction

A combined cycle (CC) concentrating solar power (CSP) plant provides significant potential to achieve an efficiency increase and an electricity cost reduction compared to current single-cycle plants. A CC CSP system requires a receiver technology capable of effectively transferring heat from concentrated solar irradiation to the pressurized air stream of a gas turbine. The small number of pressurized air receivers demonstrated to date have practical limitations when operating at high temperatures and pressures. As yet, a robust, scalable and efficient system has to be developed and commercialized. A novel receiver system, the SCRAP concept, has been proposed to comply with these requirements [1]. The SCRAP system is conceived as a solution for an efficient and robust pressurized air receiver that could be implemented in CC CSP concepts or standalone solar Brayton cycles without a bottoming Rankine cycle.

The study of pressurized air receivers is a young field of research, with a small number of receivers proposed and tested to date. It was found that a solar receiver system that provides a high solar-thermal efficiency as well as good optical efficiency (not requiring a secondary concentrator and operating with a surrounding heliostat field), is robust (not dependent on fragile materials) and operates under a low pressure drop has yet to be found [2].

2.1. The SCRAP Receiver Concept

The SCRAP receiver was conceived with the intention to overcome these challenges in an effective, robust and cost-efficient manner. It is intended as an external metallic tubular pressurized air receiver, with the purpose of pre-heating an air stream to up to 800 °C upstream of a gas turbine's combustion chamber (or secondary receiver) [3]. A representation of the receiver is shown in Fig. 1. The tubular absorber assemblies (referred to as spikes) are concentrically arranged in such that they describe a body of increasing density towards the receiver centre and allow for a receiver type that can operate with a surrounding heliostat field, leading to an increased annual optical solar field efficiency.

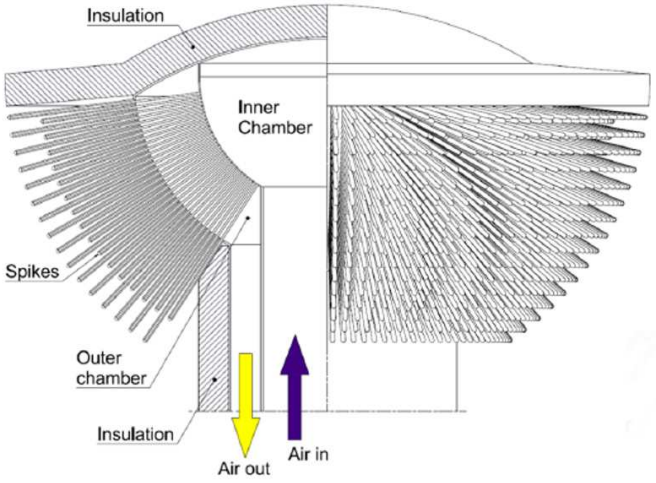

Fig. 1. A manifestation of the SCRAP receiver (left half in section) [1]

The incoming air (from the compressor) enters the receiver through an inner chamber. From there the air stream is directed through circular tubes into the absorber assemblies. Each spike (see Fig. 1) consists of two concentric tubes, of which the inner supplies the incoming air stream from the inner chamber to the spike tip (outermost point) from where the air flow is directed back by 180° towards the receiver centre, passing through the outer tube. The outer tube‘s outer surface is exposed to the concentrated irradiation and in the process heated up, transferring thermal energy to the pressurized air stream.

The temperature of the outer tube wall is intended to rise from the spike tip towards the highest temperature at the spike root (where it is mounted to the receiver structure). With radiative heat losses gaining significance at higher temperatures this surface temperature distribution becomes advantageous. As a result a macro-volumetric effect is envisaged, where the highest material temperatures occur deep within the receiver. A large cooling effect is achieved at the most exposed area, the spike tip, where relatively cool air exits the inner tube. With lower solar irradiation expected towards the spike root, the risk of the absorber pipe exceeding temperature limitations is lowered.

2.2 Previous Work

A ray-tracing study was conducted in order to understand the receiver’s sensitivity to solar field parameters. It was found that the effect of heliostat size/facet size has a notable effect on the flux distribution along a spike [3]. As the spike tip points towards the solar field it experiences the highest flux. Due to the geometry of the spike tip a strong cooling effect of the impinging air stream onto the tip surface (end cap in Fig. 1) - as it changes the flow direction by 180° - is envisaged. The heat transfer model introduced in reference [3] describes the internal heat transfer within a spike. In the model the spike tip is treated as a black box operating with an averaged Nusselt number and flux input. That model was expanded in reference [4] by adding a section representing the jet impingement cooling of the spike tip. Further, heat losses to ambient, comprising natural convection, forced convection as well as thermal radiation were implemented. The predicted solar-thermal efficiency of a SCRAP receiver spike was approximately 80 % at an air outlet temperature of 800 °C and an ambient wind speed of 3 m/s at receiver height [4].

This heat transfer model requires validation to increase confidence into the predicted receiver performance. In this paper an experimental setup that was designed, constructed and built at the heat transfer laboratory at Stellenbosch University is presented.

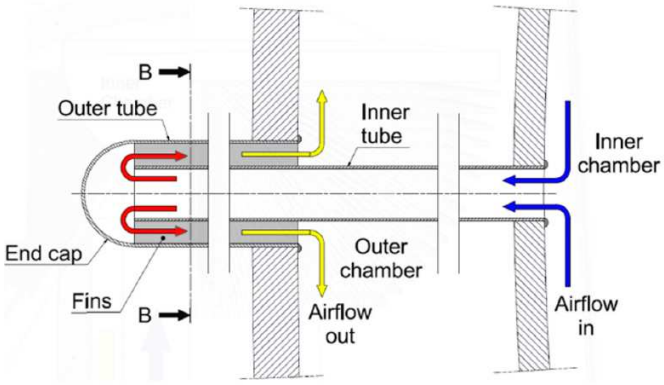

Fig. 2. Section through tube geometry [1]

3. Laboratory Test Setup

A test setup was designed, constructed and built at Stellenbosch University. The design was intended to be modular and interchangeable. This permits testing of multiple phenomena or spike components (or unrelated heat transfer experiments) in a variety of configurations. The experimental test setup is initially introduced in the configuration used to investigate pressure drop and convective heat transfer within the rectangular ducts, including sensory equipment used. The section thereafter provides details on the variability of the setup.

3.1 Description

A photograph of the test rig is shown in Fig. 3. The components are introduced, following the flow of air through the system. Pressurized air is available at an absolute pressure of

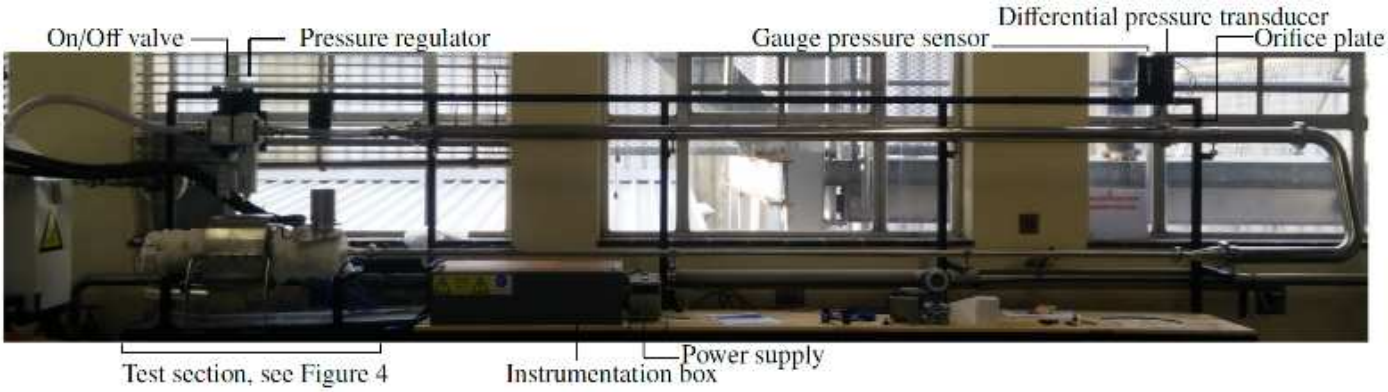

Fig. 3. Photograph of the test rig in the heat transfer laboratory

approximately 1 MPa and regulated to the desired pressure and mass flow rate. The pressurized air enters the setup through an on/off valve, shown on the top left.

Thereafter, a pressure regulator (incl. a 40 µm filter unit) permits regulation of the air pressure at a nominal air flow rate of up to 20 000 L/min [5]. The air inlet temperature is measured downstream the pressure regulator. Thereafter, an orifice plate is used to establish the mass flow rate. From the orifice plate the air stream is directed towards the test section (Fig. 4).

There, a steam compartment was built to provide thermal energy input at a constant temperature of nominally 100 °C on the outside surface of the investigated spike section. This temperature enables confirmation of convective heat transfer models, while permitting cost effective materials and manufacturing processes

In the configuration shown in Fig. 4 and Fig. 5 a 210 mm section with internal fins is heated. After the air flow exits the inner tube and is redirected by 180° towards the right it flows through an annular space. This annular section of 114 mm length is intended to reduce the flow stratification before entering the internally finned section. A short internally finned section of 114 mm length is used for the air flow within the ducts to develop and the wall friction to stabilize. Using spacers of 0.5 mm thickness, the flange is thermally insulated by an air gap towards the flange of the heated section. A 210 mm long internally finned, heated section is submerged in the steam compartment. For the length of the inner tube being within the heated internally finned section its outer diameter was reduced to provide an air gap of about 0.3 mm in order to eliminate thermal conduction from the fin tips to the inner tube.

From the downstream flange of the heated section, equally using a 0.5 mm air gap for insulation purposes, the heated air flows through an annular segment of 114 mm length. In the last segment the air flow direction is changed by 90° upwards towards the exhaust silencer. Should the temperature distribution show stratification, the duct towards the silencer can be filled with metal wool (e.g. brass or copper wool) to mix the air flow and achieve a more homogenous air temperature. An adapter flange positioned before the air exits the setup through the silencer houses three thermocouples. Each thermocouple, measuring the air outlet temperature, is inserted at different length.

In order to reduce the number of variables for a thermal experiment it was decided to develop a test setup heated by steam at ambient pressure. Therewith, the heating temperature is constant at the condensing temperature (100 °C). Measuring steam condensate mass, electric input power at the steam generators as well as the inlet and outlet temperature of the air stream provides assurance on the validity of generated data. Fig. 4 shows a photograph of the test section of the setup. The steam compartment is insulated by another steam loop through a wall cavity and therefore not additionally insulated to ambient. The steam compartment is mounted individually (mounting arms can be seen in Fig. 4) and is sealed with rubber foam towards the

Fig. 4. Test section without insulation cladding

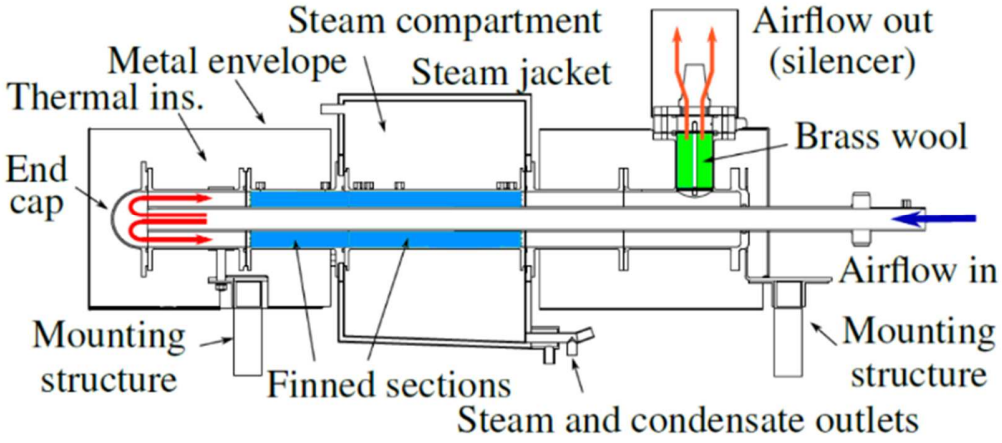

Fig. 5. Test setup in a configuration with heated internally finned section

flanges, therewith minimizing conduction between the wall and the test section.

A steam generator of 4 kW_t rating is used to provide steam for heating of the jacket. A second steam generator was upgraded to 6 kW_t rating and is used to provide steam to the steam compartment (see Fig. 5). Both steam generators are equipped with voltage regulators.

3.2. Sensor placement

The sensor placement in the test setup is introduced in the configuration shown in Fig. 4 and Fig. 5. The experiment is intended to confirm the developed simulation models to predict the performance of the SCRAP receiver. This includes the heat transfer models as well as pressure drop. To this end, several pressure taps for static pressure measurement were added. As the ducts for the air flow are narrow (3 mm) and thermocouples would influence flow profiles. To gain a reasonable resolution of temperature da ta, temperature readings are taken at various depths of the fins on different axial positions to improve insight into heat transfer characteristics. Axial sensor positioning and thermocouple insertion holes are shown exemplary in Fig. 6.

Over three axial locations the metal temperature can therewith be measured at various depths within the fins. Since the test setup is axially symmetrical, the measured data can be superimposed onto a single fin (permitting comparison to a simplified computer simulation, modelling a periodic section only).

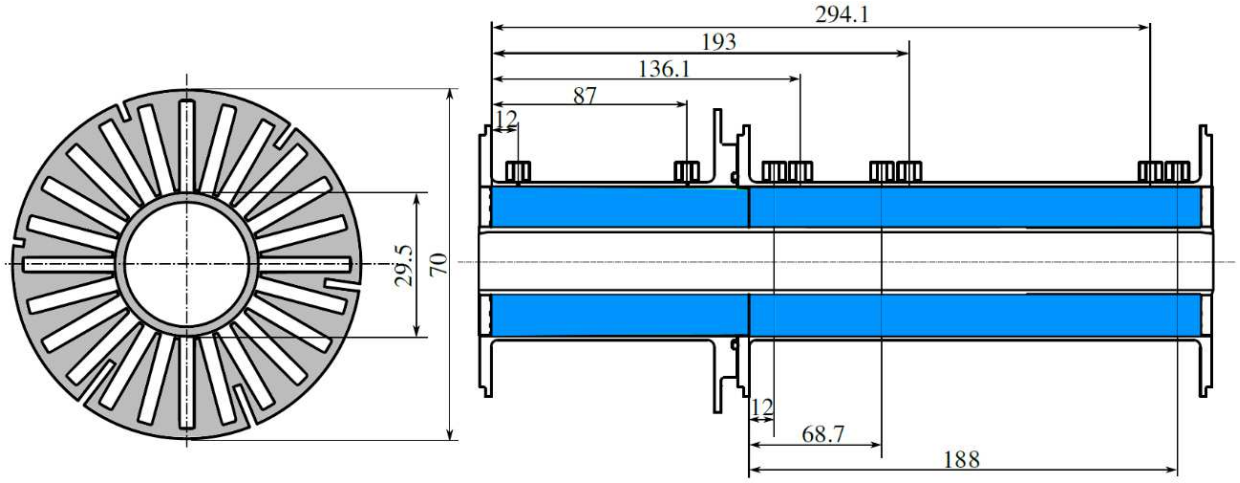

Fig. 6. Section through internally finned tube at axial position where thermocouples are inserted to depths between 2.0 mm and 10.4 mm (left), axial distance of static pressure taps to inlet into rectangular ducts above the tube, distance of thermocouple measurement points to beginning of heated section below the tube (right). Illustrations are not to scale.

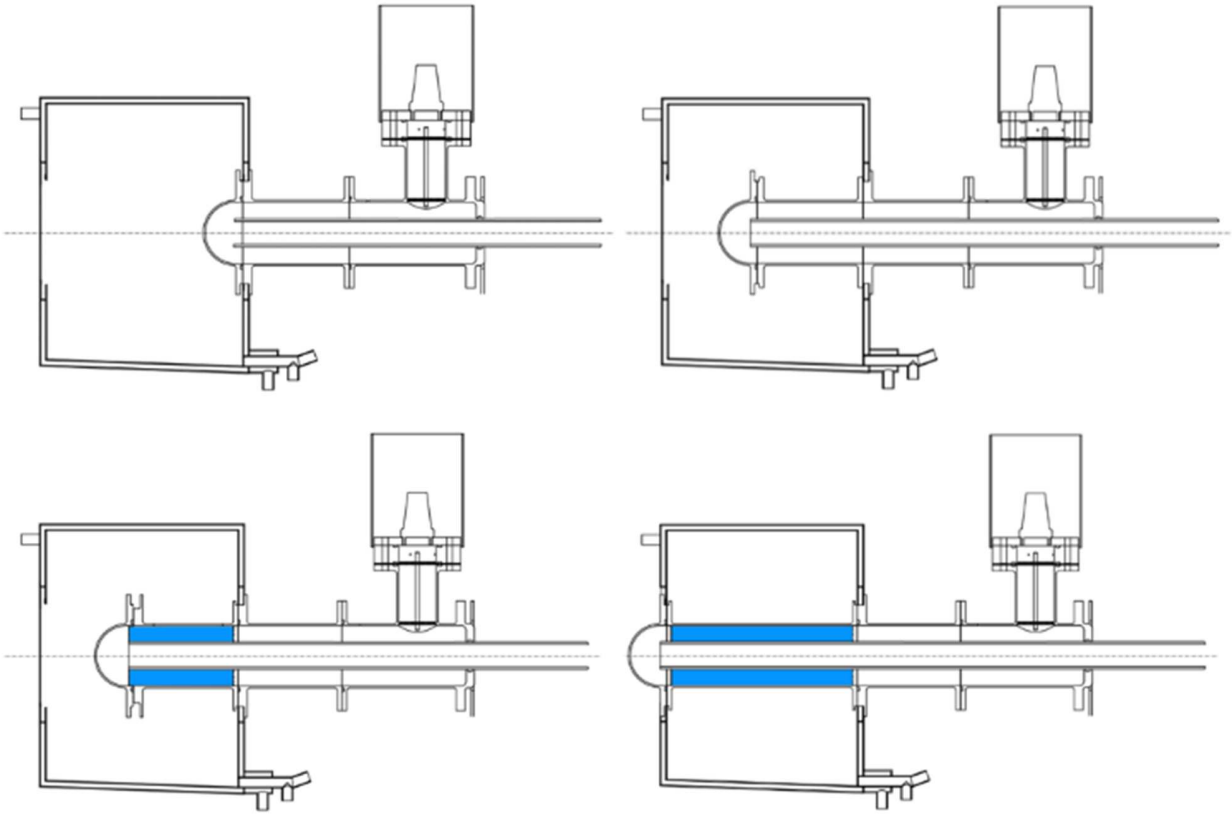

Fig. 7 Experimental configuration with tip heated (top left), tip and annular space heated (top right), tip and internally finned section heated (bottom left) and an internally finned section heated (bottom right)

3.3 Sensory equipment and calibration

Prior to conducting experiments the type-T thermocouples were calibrated using a Fluke 9142 Field Metrology Well. The differential pressure transducers (Freescale MPX2050D; differential pressure range 0 kPa – 50 kPa; linearity 0.25 % [8]) were calibrated using a Betz type 5000 Micromanometer. For the range exceeding 5000 Pa correct functionality was validated against a mercury manometer.

The gauge pressure was measured using a Firstrate FST800-10B (pressure range 0 kPa – 1000 kPa; accuracy 0.3 % [9]). Data logging is conducted using a Keysight 34970A data acquisition control mainframe with three Keysight 34907A multifunction modules [10].

4 Variable Configuration

The test setup is of modular nature in order to provide a platform enabling a variety of experiments relating to research on the SCRAP spike. For this purpose the steam compartment is mounted on rails, permitting flexible positioning thereof. Fig. 7 suggest variations of configurations foreseen to be of use when conducting experiments towards confirming modelling of the tip region with particular interest to the interaction at the tip and the inlet into the rectangular ducts.

Fig. 5 shows the test setup in a configuration intended to confirm heat transfer modelling on the internally finned tube. The blue areas mark the internally finned parts, while outer tube segments that have no colour filling are annuli.

If desired, the internally finned tubes can be replaced with other fin geometries or materials, should further work be required. Helically finned segments can be used instead of straight fins.

5 FEM Analysis

With pressures of up to 1 MPa possible during the experiments the peak stress in the internally finned sections were analysed using FEM. The peak stress occurs on the inner side of the pipe wall where stress concentration is observed on the on roots. Literature (such as [6]) does not offer a stress concentration factor directly applicable to a spike's geometry. To develop a sound understanding of stress distribution and peak stress values a minimal periodic sample was simulated in MSC Patran [7]. The sample contains half a duct including half a fin (see Fig. 8).

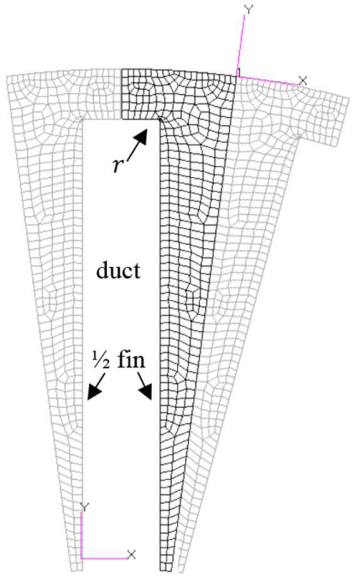

Fig. 8. Coarse mesh of half fin, two further half fins illustrated for clarity.

The simulation boundary conditions applied were edge pressure on the inside and outside walls of 1 MPa and 0.1 MPa, respectively.

The symmetric boundary condition is configured as a wall node based restriction of transversal (x-direction) movement (<0; ;>) and rotation around the axis in axial (z-) direction (<; ;0>). A coordinate system on each boundary is required to configure the boundary conditions as described (see local coordinate system on top right corner of Fig. 8).

The linear static solver is used to compute the stress. The peak stress is observed with increased mesh resolution until convergence is achieved. Increasing grid resolution was conducted by splitting each quad cell into 4 in each step, which is permissible due to the relatively small computational expense of the refined setups.

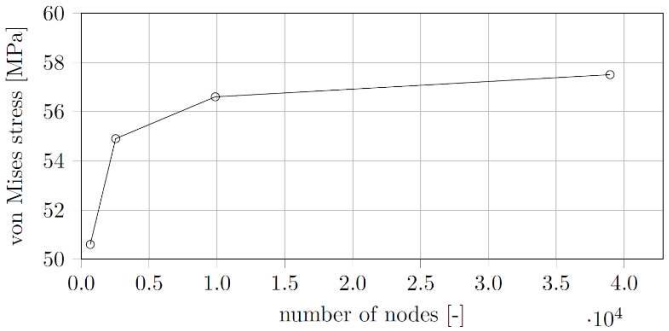

Fig. 9. Peak stress over number of nodes

The simulation was repeated with increasing grid resolution until the solution converged. The development of the peak stress over a refined grid is depicted in Fig. 9 and shows the peak stress to appear to be levelling out at about 58 MPa (here, for a radius r of 0.1 mm).

In comparison, the stress in tangential direction for a cylindrical pressure vessel (here, the tube without internal fins) is approximated with

$$\sigma_t = \frac{pr}{t}$$

where t is the wall thickness and the cylinder is assumed as thin walled. As a reference, a tube with r = 0.035 m, t = 2 mm and a pressure p of 1 MPa will result in σ_t = 15.75 MPa (assuming an external pressure of 0.1 MPa).

This case of a plain circular tube has been simulated in MSC Patran to validate the simulated result and setup. The identical case as above with p = 1 MPa and r = 35 mm and a wall thickness t = 2 mm has been configured. A 7.5° slice of the tube was meshed and the edge pressure boundary condition applied. As a result the inner wall stress $\sigma_{t,i}$ was given with 15.7 MPa, correlating well with the analytical solution of 15.75 MPa calculated.

A peak stress of about 58 MPa suggests a stress concentration factor for the rectangular duct with a 0.1 mm fillet of 3.7. This value was compared to literature values from Pikley [5] on cases that suggested some similarity.

Assuming a radius at the fin roots of 0.1 mm, the stress concentration factor K for a shoulder fillet for a stepped at tension bar under tension can be estimated in the range of $K \approx 5$. As a further reference, K for opposite deep hyperbolic notches

Fig. 10. Test section mounted in wire cutting machine

Fig. 11. Internally finned section before (left) and after wire cutting (right).

in an infinitely wide thin bar under tension can be estimated at about $K \approx 8$.

With these references in mind and considering stress concentration factors tending to be lower for multiple repeating notches as compared to a single notch it seems that the established peak stress simulated in MSC Patran is valid.

6 Manufacturing of Internally Finned Sections

The test setup is a once-off prototype. Accordingly, a manufacturing process was required that permits production in a cost-efficient manner. A machining process was required that would

- permit cutting a depth of ~200 mm,
- introduce little force or heat to avoid narrow fin tips deforming/breaking and
- provide cost effective production.

It was decided to employ an electrical discharge machining process (wire cutting) that permitted fulfilling the above requirements. With a wire diameter of 0.10 mm, a radius of r = 0.35 mm was selected for the fin roots (see Fig. 8) in order to permit the wire to cut a smooth curvature. Due to vertical space requirements for mounting brackets in the wire cutting machine a part length of ~200 mm was selected. Fig. 10 shows the test section mounted in the wire cutting machine. The spike components were manufactured from 7050 aluminum alloy.

Fig. 11 shows an internally finned section before and after wire cutting. The component shown features protruding fins in order to form a minimal air gap when connected to the heated section. As shown in Fig. 12 the beginning of the fins is recessed on the upstream as well as downstream side of the heated section in order to reduce the impact of the flange onto radial thermal conduction from the hot surface (exposed to steam) to the internal fins.

5. Conclusion

The research on the SCRAP receiver performance was expanded by introducing a modular experimental heat transfer setup in order to validate models created for the performance

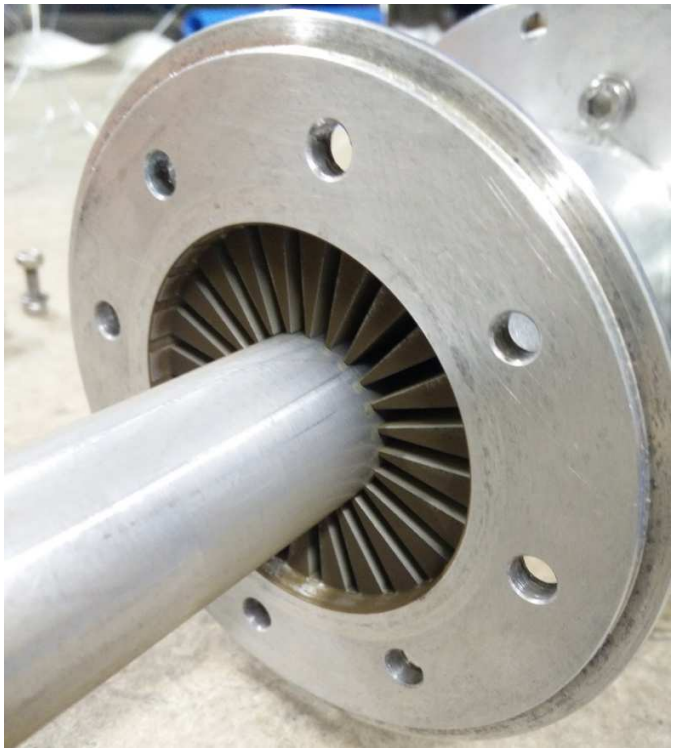

Fig. 12. Inner tube inserted into wire cut section

prediction. The test setup was designed and constructed at Stellenbosch University.

The test setup permits experimental work on the air flow and heat transfer within a SCRAP's spike. Interchangeability of the components allows for new developments to be tested.

Acknowledgements

The authors thank the Department of Mechanical and Mechatronic Engineering and the Solar Thermal Energy Research Group (STERG) at Stellenbosch University for funding of this research through the Eskom Chair in Concentrating Solar Power. Gratitude is extended to the workshop at the Department of Mechanical and Mechatronic Engineering at Stellenbosch University for advice and guidance towards realization of the experimental setup.

References

[1] D. G. Kröger, "Spiky Central Receiver Air Pre-heater (SCRAP)," Tech. Rep. (University of Stellenbosch, Stellenbosch, 2008).

[2] M. Lubkoll, T. von Backström, and D. G. Kröger, "Survey on Pressurized Air Receiver Development," in 2nd Southern African Solar Energy Conference 2014 (Port Elizabeth, 2014).

[3] M. Lubkoll, T. von Backström, T. Harms, and D. G. Kröger, Energy Procedia 69, 461–470 (2015).

[4] M. Lubkoll, T. von Backström, and T. Harms, AIP Conference Proceedings 1734, 1–7 (2016).

[5] FESTO, Filter regulators MS-LFR, MS series Filter regulators MS-LFR, MS series (FESTO).

[6] W. D. Pikley, Petterson's Stress Concentration Factors (2nd ed.). New York: John Wiley & Sons, Inc. (1997).

[7] MSC, Patran, computer software (2014)

[8] Freescale, Freescale Semiconductor MPX2050 (Freescale semiconductor, Tempe, 2008), pp. 1–9.

[9] Firstrate, FST800-211 Universal Industrial Pressure Sensor, 2016.

[10] Keysight Technologies, Keysight 34970A Data Acquisition / Switch Unit Family. Keysight Technologies. (2014).